Quantum states of a sextic potential: hidden symmetry and quantum monodromy

2000 J. Phys. A: Math. Gen. 33 5653

(http://iopscience.iop.org/0305-4470/33/32/303)

J. Phys. A: Math. Gen. **33** (2000) 5653–5661. Printed in the UK PII: S0305-4470(00)13938-1

Quantum states of a sextic potential: hidden symmetry and quantum monodromy

Mark S Child, Shi-Hai Dong and Xiao-Gang Wang
Physical and Theoretical Chemistry Laboratory, South Parks Road, Oxford OX1 3QZ, UK

Received 16 May 2000

Abstract. A known terminating polynomial ansatz for a finite sub-set of states of the sextic central potential $V(a, b, c; r) = ar^2 + br^4 + cr^6$, $c > 0$, subject to integer related parameter constraints, is confirmed to apply in two as well as three dimensions. A hidden symmetry relating the eigenstates of $V(a, b, c; r)$ to those of $V(a, -b, c; r)$ is used to establish the boundary between the ansatz sub-set and the infinite set of higher states. Connections between the radial wavefunctions $R_n(a, b, c; r)$ and $R_{n'}(a, -b, c; r)$ also provide semiclassical insight into the origin of the parameter constraint. Finally the ansatz eigenvalue dispositions are related to the phenomenon of quantum monodromy.

1. Introduction

Solutions to the Schrödinger equation for anharmonic central potentials are relevant to structural phase transitions [1], polaron formation [2], fibre optics [3] and molecular physics [4]. Certain classes of such potentials also have the interesting property that the infinite set of normalizable bound states can contain a finite sub-set representable by means of terminating polynomials [6,7] or Laurent series [8–18] provided that the potential parameters are related in a particular way. Related work [19] employs supersymmetry inspired factorizations to obtain similar results. A variety of such so-called 'ansatz' solutions have been presented [6–18], but little if any attention has been given to the nature of the boundary between this ansatz sub-set and the infinite set of higher states.

This paper concerns a hidden symmetry responsible for the above division, in the particular case of a sextic central potential

$$V(a, b, c; r) = ar^2 + br^4 + cr^6 \qquad c > 0. \tag{1}$$

Details of the ansatz are presented for two-dimensional motion in a plane, and minor differences from earlier three-dimensional results are discussed. The distinguishing feature of the ansatz states is seen to be that their wavefunctions vanish not only as $r \to \infty$, but also as $r \to \mathrm{i}\infty$, and it is this double boundary condition that imposes a constraint on the potential parameters as well as on the energy levels. The substitution $r \to \mathrm{i}r$ also demonstrates intimate connections between the energies and wavefunctions of the potential $V(a, b, c; r)$ and those for $V(a, -b, c; r)$, with the sign of b reversed. It is interesting to note the known existence of a possibly related symmetry under the substitution $r \to r^{-1}$ for certain inverse anharmonic potentials [17], but any connection with the present work remains to be established.

The paper starts with a presentation of the ansatz in section 2. The following section explores the hidden symmetry between the eigenvalues $E_n(a, b, c)$ and $E_{n'}(a, -b, c)$, and the corresponding wavefunctions. Further insight is provided in section 4 by employing a

0305-4470/00/325653+09$30.00

double semiclassical quantization condition on $R_n(a, b, c; r)$ and its analytic continuation $R_n(a, b, c; \mathrm{i}r)$. As a by-product, the ansatz analysis allows the construction of a range of angular momentum states for given potential parameters (a, b, c) and section 5 gives a brief account of the resulting joint energy and angular momentum spectrum, under the heading quantum monodromy [4, 5]. Finally the main conclusions are collected and discussed in section 6.

2. The wavefunction ansatz

The analysis below follows the ansatz of earlier authors [6, 7], except that the motion is restricted to two rather than three dimensions. Minor differences from the earlier results will be indicated.

Solutions to the Schrödinger equation

$$\left[-\frac{1}{2r}\frac{\mathrm{d}}{\mathrm{d}r}\left(r\frac{\mathrm{d}}{\mathrm{d}r}\right)+\frac{m^2}{2r^2}+ar^2+br^4+cr^6\right]R(r)=ER(r) \tag{2}$$

are sought in the form

$$R(a,b,c;r)=\exp[-(\tfrac{1}{4}\alpha r^4+\tfrac{1}{2}\beta r^2)]\sum_{k=0}^{\infty}d_k r^{2k+|m|} \tag{3}$$

with

$$\alpha=\sqrt{2c}\qquad \beta=\frac{b}{\sqrt{2c}}. \tag{4}$$

The coefficients d_k may be verified to satisfy the three-term recurrence relation

$$A_k d_k+(B_{k+1}-E)d_{k+1}+C_{k+2}d_{k+2}=0 \tag{5}$$

where

$$A_k=-\frac{b^2}{4c}+a+\sqrt{2c}(2k+|m|+2) \tag{6}$$

$$B_k=\frac{b}{\sqrt{2c}}(2k+|m|+1) \tag{7}$$

$$C_k=-2k(k+|m|). \tag{8}$$

The physical solutions of (5)–(8), with real E, require that $A_{k-1}C_k>0$ for all relevant k, because the matrix equivalent can then be reduced to a real symmetric form by the substitution

$$d_k=\sqrt{\frac{A_{k-1}}{C_k}\frac{A_{k-2}}{C_{k-1}}\cdots\frac{A_0}{C_1}}d'_k. \tag{9}$$

However, $C_k<0$ for all k, while A_k becomes positive for sufficiently large k, unless the series is truncated by the condition $A_N=0$. The physical validity of equation (3) therefore requires the following constraint on the potential parameters:

$$a=\frac{b^2}{4c}-\sqrt{2c}(2N+|m|+2) \tag{10}$$

in which case equation (5) is equivalent to the eigensystem

$$\begin{pmatrix} B_0, & C_1, & 0, & 0 & \cdot & \cdot & 0\\ A_0, & B_1, & C_2 & & & & 0\\ 0 & A_1, & B_2, & C_3 & & & 0\\ & & & & & & \cdot\\ & & & & & & \cdot\\ 0, & 0, & 0, & \cdot & \cdot & A_{N-1}, & B_N \end{pmatrix}\begin{pmatrix} d_0\\ d_1\\ d_2\\ \cdot\\ \cdot\\ d_N \end{pmatrix}=E\begin{pmatrix} d_0\\ d_1\\ d_2\\ \cdot\\ \cdot\\ d_N \end{pmatrix} \tag{11}$$

or

$$H(a, b, c)\boldsymbol{d} = E\boldsymbol{d}. \tag{12}$$

The remaining coefficients d_k for $k = N + 1, N + 2, \ldots, \infty$ are set to zero.

Equations (4)–(12) differ from the three-dimensional results of Bose and Varma [7] only by the presence of $|m|$ in place of $(\ell + \frac{1}{2})$ in equations (6)–(8) and by factors of 2 in the definitions of the potential parameters (a, b, c) and E, arising from the fact that Bose and Varma [7] omitted factors of one-half from the kinetic energy terms in equation (2). Note also that parameter sets constrained by (10) allow the construction of $(N_0 - |m|/2 + 1)$ ansatz states with even m values, where $N_0 + 1$ is the number for $m = 0$. Generic patterns in the resulting eigenvalues are discussed in section 4.

The main point of this paper is to understand the seemingly arbitrary place of the above finite sub-set of ansatz states within the infinite bound state spectrum. For example, there appears at first sight to be nothing to explain the division between the ansatz eigenvalues, represented by heavy lines in figure 1, and the higher dashed eigenvalues obtained by diagonalization in a degenerate harmonic oscillator basis [4]. Results are presented for the four different sign combinations of parameters a and b, consistent with equation (10). An apparently unrelated observation is that figure 1(d) shows no evidence of the interleaving of levels with $E > 0$ expected from the existence of two well separated potential minima. The reason is that the lowest non-ansatz states shown occur in close lying pairs which are degenerate within six-figure accuracy for the levels shown. The following sections reveal a hidden symmetry responsible for these numerical findings.

3. Hidden symmetry

Equation (3) shows that the ansatz functions vanish not only as $r \to \infty$ but also as $r \to \mathrm{i}\infty$, and this additional boundary condition lies at the heart of the hidden symmetry. Notice for example that the substitution $r \to \mathrm{i}r$ reverses the signs of b and E in (2), leaving the remaining parameters invariant; and comparison between figures 1(a) and (b) (or figures 1(c) and (d)) confirms that the uppermost ansatz level $E_N(a, b, c)$ is indeed the negative of the ground state $E_0(a, -b, c)$ when the sign of b is reversed. In other words the ansatz eigenvalues $E_n(a, b, c)$ are bounded above by the negative of $E_0(a, -b, c)$.

To explore the connection in another way, suppose that

$$H(a, b, c)\boldsymbol{d}_n = E_n(a, b, c)\boldsymbol{d}_n \tag{13}$$

and consider the effect of the substitution $b \to -b$. It follows from equations (4)–(8) that $\beta \to -\beta$ and $B_k \to -B_k$, while $\alpha \to \alpha$, $A_k \to A_k$ and $C_k \to C_k$. Thus, in view of the tridiagonal nature of equation (11),

$$H(a, -b, c)\hat{\boldsymbol{d}}_n = -E_n(a, b, c)\hat{\boldsymbol{d}}_n \tag{14}$$

where alternate components of $\hat{d}_n$ are sign reversed with respect to $\boldsymbol{d}_n$, i.e. $\hat{d}_{nk} = (-1)^k d_{nk}$.

In other words the ordering of the eigenvalues is simply reversed so that $-E_n(a, b, c)$ corresponds to the $(N - n)$th eigenvalue of $H(a, -b, c)$;

$$E_{N-n}(a, -b, c) = -E_n(a, b, c). \tag{15}$$

The form of the corresponding wavefunction follows from equations (3) and (4)

$$\begin{aligned} R_{N-n}(a, -b, c; r) &= \exp[-(\tfrac{1}{4}\alpha r^4 - \tfrac{1}{2}\beta r^2)] \sum_{k=0}^{N} \hat{d}_{nk} r^{2k+|m|} \\ &= \exp[-(\tfrac{1}{4}\alpha r^4 - \tfrac{1}{2}\beta r^2)] \sum_{k=0}^{N} (-1)^k d_{nk} r^{2k+|m|}. \end{aligned} \tag{16}$$

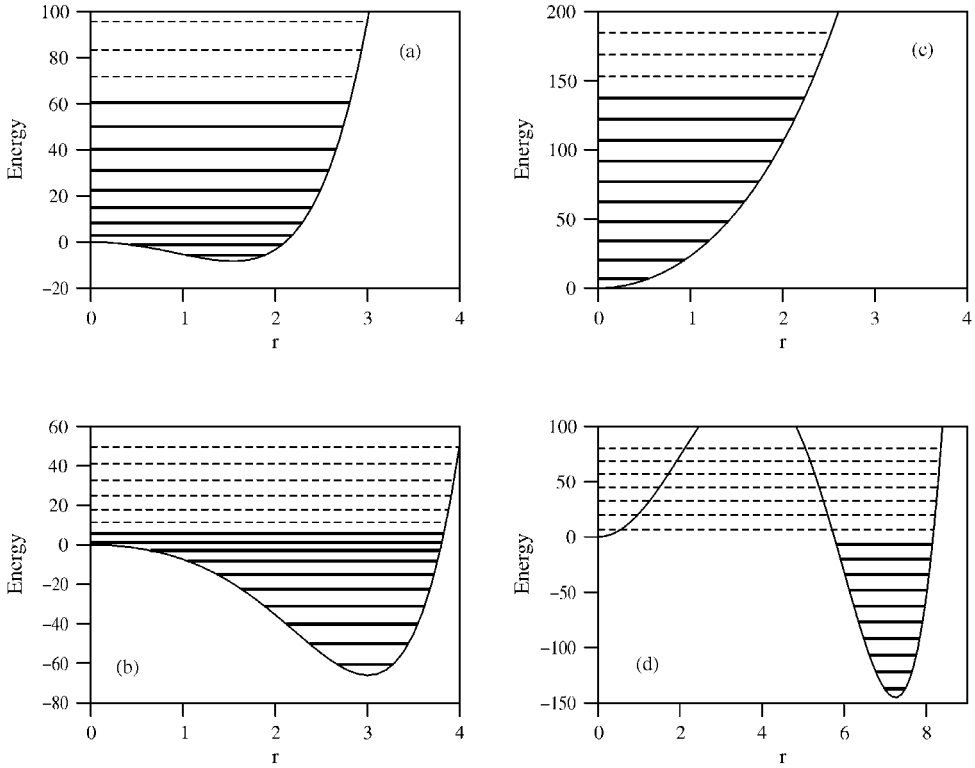

Figure 1. Low-lying zero-angular-momentum eigenvalues for (*a*) $a = -6.44$, $b = 1.0$, $c = 0.1$, (*b*) $a = -6.44$, $b = -1.0$, $c = 0.1$, (*c*) $a = 22.17$, $b = 1.0$, $c = 0.01$, and (*d*) $a = 22.17$, $b = -1.0$, $c = 0.01$. Heavy lines mark the ten ansatz eigenvalues for these parameter combinations.

Finally it follows by comparison with (16) and the analytical continuation of (3) that

$$R_{N-n}(a, -b, c; r) = R_n(a, b, c; \mathrm{i}r). \tag{17}$$

Equations (15) and (17) embody the hidden symmetry of the ansatz states, which is strikingly displayed in figure 2, by plotting $R_n(a, b, c; r)$ and their analytic continuations $R_n(a, b, c; \mathrm{i}r)$ as functions of $z = r^2$, for the four cases illustrated in figure 1.

Separate normalizations were applied over positive and negative z ranges, in order to match the oscillation amplitudes to the energy spacings. The calculations were all performed for $N = 9$ and each wavefunction displays a total of nine nodes, summed over positive and negative ranges of z, although in certain cases the spacing close to $z = 0$ is too small for graphical resolution. The inversion symmetry between figures 2(*a*) and (*b*) and figures 2(*c*) and (*d*) is a pictorial manifestation of equations (15) and (17).

4. Semiclassical quantization

Figure 2 also has a semiclassical interpretation, in the sense that the wavefunction oscillations are restricted to regions where the classical coordinates and momentum are either both real or both imaginary, giving two real action integrals. It is therefore illuminating to interpret the ansatz constraint (10) and the resultant hidden symmetry as a consequence of simultaneous quantization for $R_n(a, b, c; r)$ and its analytical continuation $R(a, b, c; \mathrm{i}r)$.

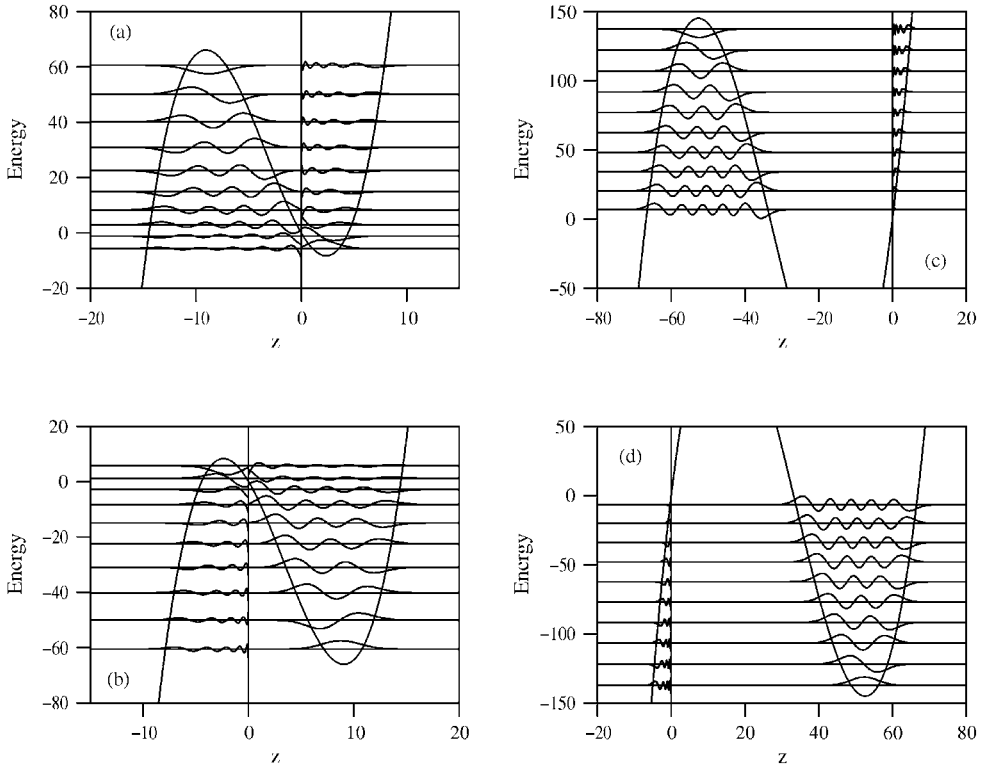

Figure 2. Ansatz wavefunctions for the parameter values in figure 1, presented as functions of $z = r^2$. The hidden symmetry with respect to the transformations $z \to -z$, $E \to -E$ and $b \to -b$ is clearly displayed.

The four turning points for the ansatz states in figure 2(*a*) are labelled $z_1 > z_2 \geqslant 0 \geqslant z_3 > z_4$ with corresponding coordinates r_i, and the relevant Bohr quantization integrals are taken as

$$I = \int_{r_2}^{r_1} \sqrt{2(E - ar^2 - br^4 - cr^6) - \tfrac{m^2}{r^2}}\, \mathrm{d}r$$
$$= \frac{1}{2}\int_{z_2}^{z_1} \frac{\sqrt{2(Ez - az^2 - bz^3 - cz^4) - m^2}}{z}\, \mathrm{d}z \tag{18}$$

and

$$J = -\frac{1}{2}\int_{z_4}^{z_3} \frac{\sqrt{2(Ez - az^2 - bz^3 - cz^4) - m^2}}{z}\, \mathrm{d}z. \tag{19}$$

The negative sign is introduced in equation (19) to ensure that $J > 0$ because $z < 0$ for $z_4 < z < z_3$.

The direct evaluation of I and J in terms of elliptic integrals leads to awkward manipulations, but it is sufficient for present purposes to note that [20]

$$\left(\frac{\partial I}{\partial E}\right)_m = \frac{1}{2\sqrt{2c}}\int_{z_2}^{z_1} \frac{\mathrm{d}z}{\sqrt{(z_1 - z)(z - z_2)(z - z_3)(z - z_4)}} = gK(k) \tag{20}$$

while

$$\left(\frac{\partial J}{\partial E}\right)_m = -\frac{1}{2\sqrt{2c}}\int_{z_4}^{z_3} \frac{\mathrm{d}z}{\sqrt{(z_1 - z)(z_2 - z)(z_3 - z)(z - z_4)}} = -gK(k) \tag{21}$$

where $k^2 = [(z_1 - z_2)(z_3 - z_4)/(z_1 - z_3)(z_2 - z_4)]$, $g = 2/\sqrt{(z_1 - z_3)(z_2 - z_4)}$ and $K(k)$ is the complete elliptic integral of the first kind [20]. It follows on integrating the sum of equations (20) and (21) that

$$I + J = K = \text{const.} \tag{22}$$

Moreover, the constant may be evaluated by choosing the energy such that $z_3 = z_4$ and $J = 0$, in which case [21]

$$\begin{aligned} I &= \frac{\sqrt{2c}}{2}\int_{z_2}^{z_1} \frac{\sqrt{(z_1 - z)(z - z_2)}(z - z_3)}{z}\,\mathrm{d}z \\ &= \frac{\pi\sqrt{2c}}{16}[(z_1 - z_2)^2 - 4[(z_1 + z_2) - 2\sqrt{z_1 z_2}]z_3]. \end{aligned} \tag{23}$$

Finally I may be expressed in terms of the potential parameters by use of the following identities for the roots of the quartic polynomial when $z_3 = z_4$:

$$z_1 + z_2 + 2z_3 = -\left(\frac{b}{c}\right) \tag{24}$$

$$z_1 z_2 + 2(z_1 + z_2) + z_3^2 = a/c = \frac{b^2}{4c^2} - \frac{2}{\sqrt{2c}}(2N + |m| + 2) \tag{25}$$

$$z_1 z_2 z_3^2 = m^2. \tag{26}$$

It is readily shown by combining equations (23)–(26) that

$$I + J = \pi(N + 1) \tag{27}$$

remembering of course that $J = 0$ when (24)–(26) apply. Given the real quantization condition [22]

$$I = (n + \tfrac{1}{2})\pi \tag{28}$$

equation (27) requires that

$$J = (N - n + \tfrac{1}{2})\pi \tag{29}$$

which is clearly consistent with the labelling in equation (17) and with the plots in figure 2.

The remarkable feature of these results is that the frequencies $(\partial E/\partial I)_m$ and $(\partial E/\partial J)_m$ of the two classical oscillators are identical for common (E, m) values for any sextic form $V = ar^2 + br^4 + cr^6$, and that simultaneous quantization leads directly to the parameter constraint (10). It is interesting to note that the same reasoning can also be applied in three space dimensions, provided that the Langer substitution [22,23] $\ell(\ell+1) \rightarrow (\ell+\frac{1}{2})^2$ is applied. The effect is to replace m^2 by $(\ell+\frac{1}{2})^2$ in equations (18), (19) and (26), while $|m|$ in equation (25) changes to $\ell + \frac{1}{2}$ in accordance with the three-dimensional variant of equation (10) given by Bose and Varma [7].

An interesting slant on the hidden symmetry may also be obtained by reversing the semiclassical argument. Suppose for example that N in equations (10) and (25) were taken to be arbitrary. The simultaneous quantization of I and J required to satisfy the boundary conditions $R(z) \rightarrow 0$ as $z \rightarrow \pm\infty$ can apply only for integer N. Hence the additional boundary condition at $z \rightarrow -\infty$ requires that the parameter a must be 'quantized' by equation (10), in addition to the normal energy quantization.

A minor extension of the above reasoning also explains the close energy degeneracies between the pairs of low-lying positive energy states in figure 1(d). The analogue of J becomes

$$J' = \frac{1}{2}\int_{z_4}^{z_3} \frac{\sqrt{2(Ez - az^2 - bz^3 - cz^4) - m^2}}{z}\,\mathrm{d}z \tag{30}$$

without the negative sign because now $z > 0$ in the range $z_4 < z < z_3$. Thus

$$\frac{\mathrm{d}J'}{\mathrm{d}E} = \frac{\mathrm{d}I}{\mathrm{d}E} \tag{31}$$

which means that the level spacings in the inner and outer wells are precisely equal. Moreover

$$I - J' = \pi(N + 1) \tag{32}$$

by extension of equation (27), so that quantization in the inner well

$$J' = (n_{\mathrm{inner}} + \tfrac{1}{2})\pi \tag{33}$$

requires simultaneously that

$$I = (n_{\mathrm{outer}} + \tfrac{1}{2})\pi$$

with

$$n_{\mathrm{outer}} = N + n_{\mathrm{inner}} + 1. \tag{34}$$

5. Quantum monodromy

It was noted in section 2 that any parameter set constrained by equation (10) implies the existence of $N_0 - |m|/2 + 1$ ansatz states for even values of $|m|$, where $N_0 + 1$ is the number for $m = 0$. Moreover the ansatz energy range for $a < 0$ necessarily includes the point $(m, E) = (0, 0)$ (see figures 1(*a*) and (*b*)), which is known to be critical for the observation of quantum monodromy in the eigenvalue spectrum of any cylindrically symmetric system with a locally quadratic maximum [4]. The classical origin of this phenomenon arises from non-analyticity in the action integral at $(m, E) = (0, 0)$, which results in a topological obstruction to the global construction of classical action-angle variables [24].

Other consequences for the joint spectrum are illustrated in figure 3, using parameters chosen to place the critical point at the centre of the diagram. One observation concerns changes in the shapes of the dashed and continuous joining curves above and below the origin. The latter, which join points of common radial quantum number n in the notation of equations (13)–(17), are seen to cross the line $m = 0$ smoothly for $E < 0$ but to take on a kink for $E > 0$. Similarly the dashed curves, which link points of common $2n + |m|$, are smooth for $E > 0$ and kinked for $E < 0$. Non-analyticity in the relevant action integral is responsible for the dislocation in each case.

The dislocations also have consequences for the parallel transport around the origin of any vector on the lattice of quantum numbers. As shown elsewhere [5, 24] any vector $(\Delta m, \Delta n)$ returns to $(\Delta m', \Delta n')$ such that

$$\begin{pmatrix} \Delta m' \\ \Delta n' \end{pmatrix} = \begin{pmatrix} 1 & 0 \\ 1 & 1 \end{pmatrix} \begin{pmatrix} \Delta m \\ \Delta n \end{pmatrix}$$

because, in semiclassical terms, parallel transport entails a switch from one sheet of the classical action integral to the next [5].

Since the current literature on quantum monodromy is largely couched in semiclassical terms [4,5,24–27], it is hoped that the present finite matrix representation will add insight into the purely quantum mechanical origin of this interesting phenomenon.

6. Summary and conclusion

An existing ansatz for finite sub-sets of states of a sextic central potential was shown to apply in two as well as three dimensions, provided that the potential coefficients (a, b, c) were subject to

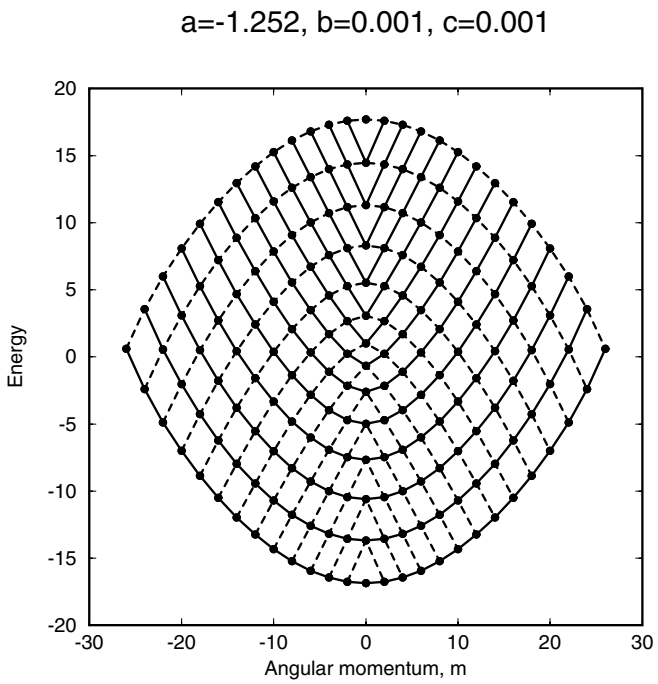

Figure 3. Quantum monodromy for $a < 0$, illustrated by the eigenvalue distribution of the ansatz states for $a = -1.252$, $b = 0.001$ and $c = 0.001$. Solid and dashed lines join points of common n and $2n + |m|$ respectively.

an integer related constraint. An analytic continuation argument was used to establish that the boundary between this sub-set and the infinite set of higher normalizable sets was attributable to a hidden symmetry, such that the ansatz eigenvalues $E_n(a, b, c)$ of $V(a, b, c; r)$ are bounded above by the negative of the lowest eigenvalue, $E_0(a, -b, c)$, of the potential $V(a, -b, c; r)$, with the quartic potential coefficient reversed. Implied connections between the wavefunctions $R_n(a, b, c; r)$ and their analytic continuations $R_n(a, b, c; \mathrm{i}r)$, were presented. The origin of the integer related (i.e. quantized) potential parameter constraint was also intrepreted by Bohr quantization techniques. Finally the relevance of the ansatz wavefunction construction to the recently studied phenomenon of quantum monodromy was indicated.

Acknowledgments

Two of the authors (Shi-Hai Dong and Xiao-Gang Wang) are grateful for support from the Royal Society of London. The encouragement of Professor Zhong-Qi Ma is also gratefully acknowledged.

References

[1] Share A and Bedra S N 1980 *Pramana J. Phys.* **14** 327
[2] Emin D 1982 *Phys. Today* **35** June 34
Emin D and Holstein T 1976 *Phys. Rev. Lett.* **36** 323
[3] Hashimoto H 1979 *Int. J. Electron.* **46** 125
Hashimoto H 1980 *Opt. Commun.* **32** 383

[4] Child M S 1998 *J. Phys. A: Math. Gen.* **31** 657
[5] Child M S, Weston T and Tennyson J 1999 *Mol. Phys.* **96** 371
[6] Kaushal R S 1989 *Phys. Lett.* A **142** 57
[7] Bose S K and Varma N 1990 *Phys. Lett.* A **147** 85
[8] Kaushal R S 1991 *Ann. Phys., NY* **206** 90
[9] Kaushal R S and Parashar D 1992 *Phys. Lett.* A **170** 335
[10] Bose S K 1994 *Nuovo Cimento* B **109** 1217
[11] Özcelik S and Simsek M 1991 *Phys. Lett.* A **152** 145
[12] Simsek M and Özcelik S 1994 *Phys. Lett.* A **186** 35
[13] Dong Shi-Hai and Ma Zhong-Qi 1998 *J. Phys. A: Math. Gen.* **31** 9855
[14] Dong Shi-Hai, Ma Zhong-Qi and Esposito G 1999 *Found. Phys. Lett.* **12** 465
[15] Dong Shi-Hai 2000 Exact solution of the Schrödinger equation with the inverse-power potential in 2D, in preparation
[16] Znojil M 1989 *J. Math. Phys.* **30** 23
[17] Znojil M 1990 *J. Math. Phys.* **31** 108
[18] Znojil M 1982 *J. Phys. A: Math. Gen.* **15** 2111
[19] Adhikari R, Dutt R and Varshni Y P 1989 *Phys. Lett.* A **141** 1
[20] Byrd P F and Friedman M D 1954 *Handbook of Elliptic Integrals for Engineers and Physicists* (Berlin: Springer)
[21] Grodsteyn I S and Ryzhik I M 1994 *Table of Integrals, Series and Products* 5th edn (New York: Academic)
[22] Child M S 1991 *Semiclassical Mechanics with Molecular Applications* (Oxford: Oxford University Press)
[23] Langer R E 1937 *Phys. Rev.* **51** 669
[24] Bates L R 1991 *J. Appl. Math. Phys. (ZAMP)* **42** 837
[25] Ngoc S V 1999 *Commun. Math. Phys.* **203** 465
[26] Cushman R H and Sadovskii D A 1999 *Europhys. Lett.* **47** 1
[27] Sadovskii D A and Zhilinski B I 1999 *Phys. Lett.* A **256** 235